

Vibrational Spectroscopic Studies of L-Ascorbic Acid and Sodium Ascorbate

JAN HVOSLEF and PETER KLÆBOE

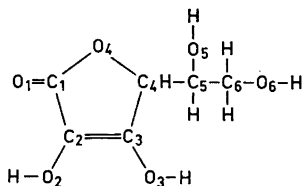
Department of Chemistry, University of Oslo, Blindern, Oslo 3, Norway

The infrared spectra of crystalline L-ascorbic acid, deuterated L-ascorbic acid, and sodium ascorbate were recorded in the region 4000–200 cm^{-1} . Raman spectra of the samples as solids and as saturated aqueous solutions were obtained.

The vibrational spectra of the crystalline solids have been discussed in terms of the known structural parameters, previously determined by diffractational analyses. Particularly, the observed O–H and O–D stretching frequencies have been correlated with the O···O distances with various degrees of hydrogen bonding. Various changes were observed in the Raman spectra upon solution of these substances in water, but no drastic rearrangements occurred.

The exchange of H by D atoms in the hydroxyl positions obtained by repeatedly dissolving L-ascorbic acid in D_2O was roughly equal to that found in a previous neutron diffraction analysis and did not exceed 60 % exchange.

The present work had various purposes. We wanted primarily to record complete infrared and Raman spectra of ascorbic acid (Vitamin C), henceforth called HASC, and sodium ascorbate (NaASC).



Their crystal structures have recently been determined,^{1,2} and for HASC even a neutron diffraction study has been performed.³ Therefore a correlation between their vibrational spectra and structures seemed feasible. Moreover Raman spectroscopic technique allows us to compare solids with aqueous

solutions of these compounds. Thus, it should be possible to establish whether the molecular structures of HASC and ASC^- as determined in the crystalline state¹⁻³ were maintained in aqueous solution. By varying the pH in solution, the protolytic equilibrium between the free ascorbic acid and its monovalent anion (ASC^-) was studied and the Raman bands assigned to each species observed simultaneously. Previously, HASC and certain derivatives have been studied by infrared⁴⁻⁷ and Raman⁸ spectroscopic technique.

EXPERIMENTAL

Chemicals. The ascorbic acid and its sodium salt were commercial products (*p.a.*) from Merck and they were not purified further.

Deuterated HASC was prepared by dissolving the substance in heavy water (98.4 % D_2O) and evaporating it to dryness during 1–2 h. This procedure was repeated three times. Infrared spectra of the solid were recorded and compared with the spectrum of the normal acid.

Instrumental. The infrared spectra were recorded with a Perkin-Elmer model 225 spectrometer. The solid compounds were studied as Nujol mulls and as KI and CsI pellets in the region 4000–200 cm^{-1} .

Raman spectra were obtained with the aid of a Cary 81 spectrometer, equipped with a Spectra Physics model 125 helium-neon laser. The crystalline samples were placed in a cylindrical sample tube of pyrex glass and the flat bottom was placed in contact with the hemispherical lens. Various saturated solutions of HASC and NaASC in water were prepared: (a) HASC in water; (b) HASC in water in which pH was adjusted to 0 by adding HCl; (c) NaASC in water; (d) NaASC in water in which pH was adjusted to 9 by adding NaOH; and (e) HASC in water with pH adjusted to 4.2 by adding NaOH. These solutions were filled into the standard silica capillary cells and the Raman spectra recorded in the axial illumination.

RESULTS AND DISCUSSION

The infrared spectra of HASC, deuterated HASC and NaASC as KI tablets are shown in Figs. 1, 2, and 3, respectively. Raman spectra of solid HASC and NaASC are given in Figs. 4 and 5 whereas the aqueous solution spectra of these molecules are shown in Figs. 6 and 7. The frequencies for the undeuterated molecules are listed in Table 1.

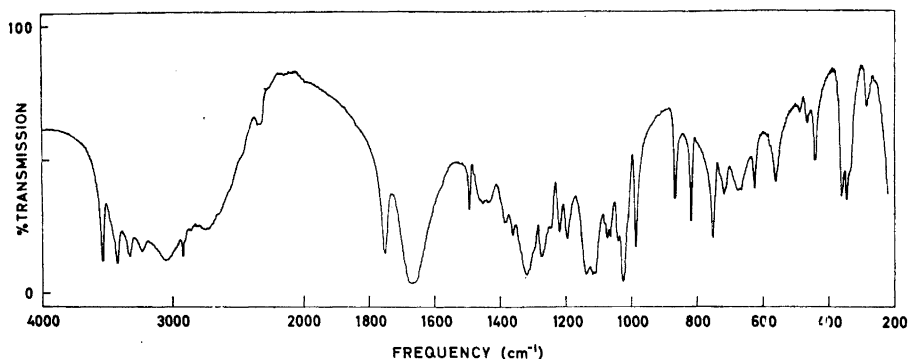


Fig. 1. The infrared spectrum of solid L-ascorbic acid (KI-pellet).

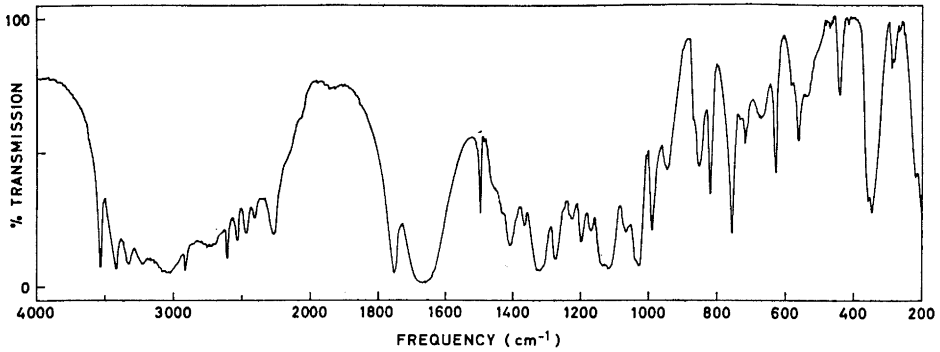


Fig. 2. The infrared spectrum of deuterated L-ascorbic acid (KI-pellet).

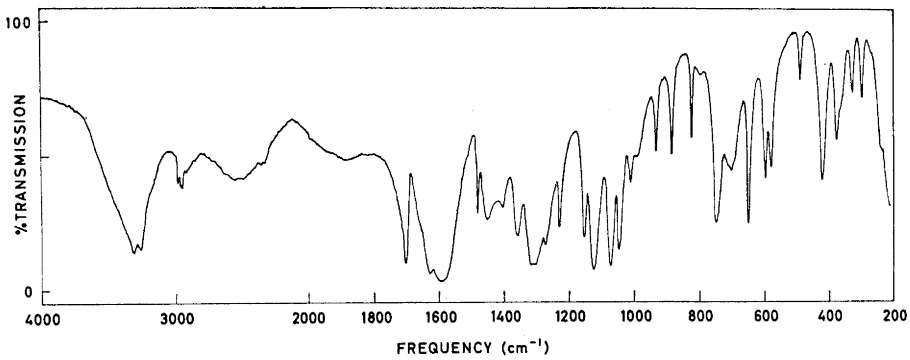


Fig. 3. The infrared spectrum of solid sodium ascorbate (KI-pellet).

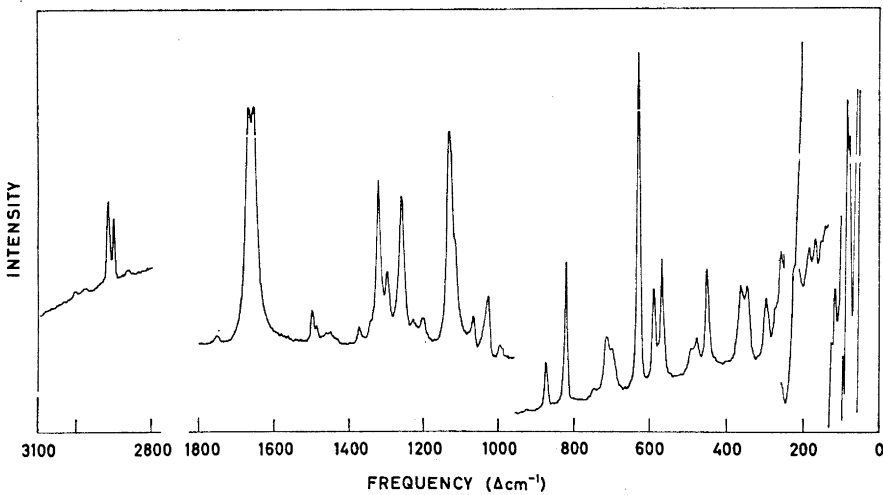


Fig. 4. The Raman spectrum of solid L-ascorbic acid.

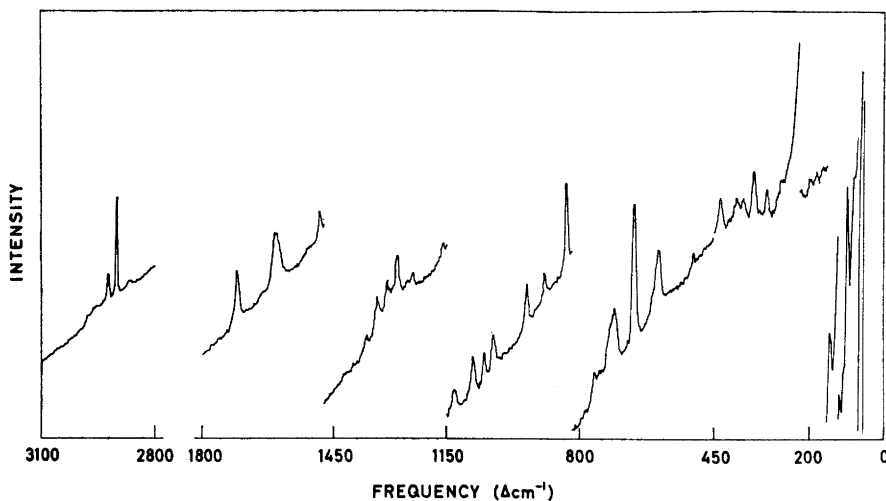


Fig. 5. The Raman spectrum of solid sodium ascorbate.

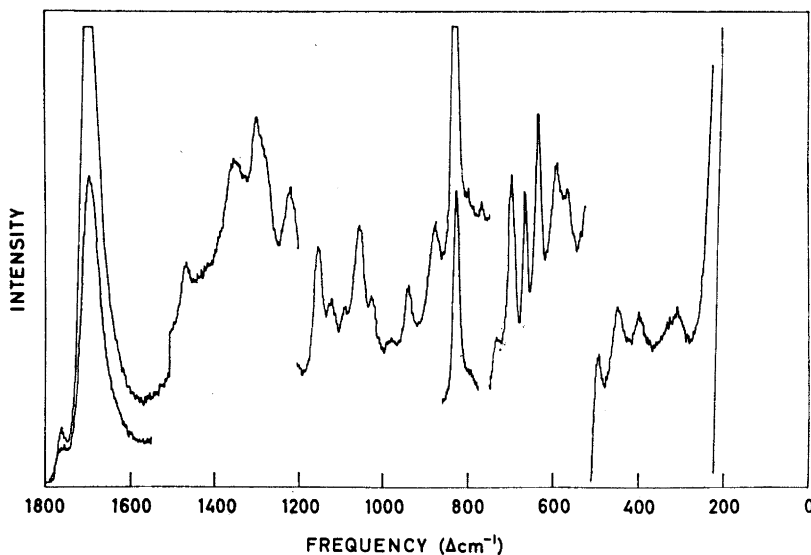


Fig. 6. The Raman spectrum of L-ascorbic acid in aqueous solution (saturated).

Obviously, HASC and NaASC are far too large and unsymmetrical molecules to warrant any detailed interpretation of the spectra. In the frequency region above 1200 cm^{-1} the vibrational bands may as a first approximation be interpreted as localized vibrations involving O-H, C-H, C=O or C=C, while the low frequency stretching and bending modes are highly mixed and involve the whole molecule.

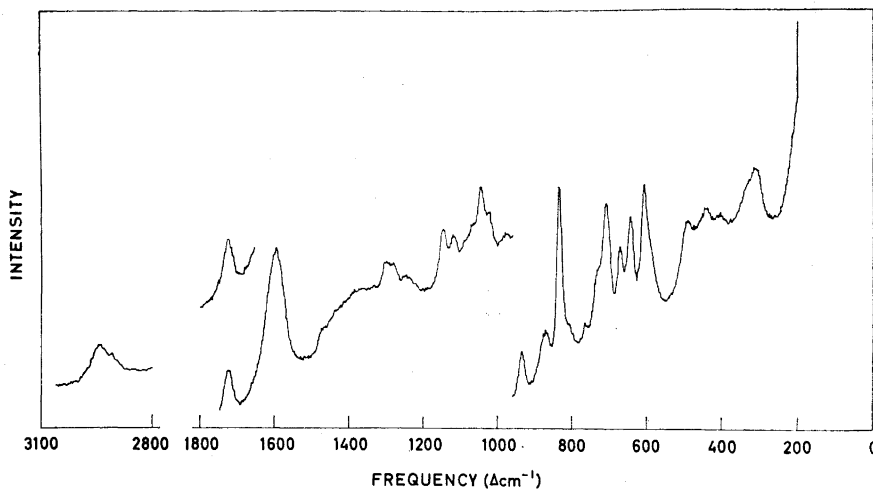


Fig. 7. The Raman spectrum of sodium ascorbate in aqueous solution (saturated).

It appears from Figs. 1, 3, 4, and 5 and from Table 1 that the infrared and Raman spectra of HASC and NaASC in the solid state are closely related in the high frequency range. In the low frequency region the spectra are quite different, in agreement with the structural and conformational differences between HASC and NaASC in the solid.¹⁻³ Additional support for the conformational differences in the lactone rings of HASC and ASC⁻ in solution has recently been obtained by studies of circular dichroism.⁹

Spectra of the solids

O-H stretching region. It is well known that a free hydroxyl group gives rise to a vibrational band around 3650 cm^{-1} , but the position and intensity of this band is highly influenced by hydrogen bonding.¹⁰ Particularly, the infrared absorption band has been extensively employed to study hydrogen bonding, and various correlations have been proposed¹¹ between the frequency shift ($\Delta\nu_{\text{OH}}$) and the hydrogen bond enthalpy ($-\Delta H^\circ$). Since the $\text{O}\cdots\text{H}$ and the $\text{O}\cdots\text{O}$ distances are related to the hydrogen bond energy, the latter distance can be correlated with ν_{OH} ¹² or $\Delta\nu_{\text{OH}}$.¹³

It appears from Fig. 1 and Table 1 that five infrared absorption bands were observed above 3000 cm^{-1} in HASC, all of them presumably associated with hydrogen bonded O-H stretching. The infrared bands at 2915 and 2860 cm^{-1} are definitely C-H stretching bands, but in addition the weak band at 2740 has been correlated with a strongly hydrogen bonded O-H stretching vibration. There are two non-equivalent molecules in the unit cell of HASC^{1,3} and eight intermolecular $\text{O}-\text{H}\cdots\text{O}$ bonds, for which the bond lengths revealed various degrees of hydrogen bonding. The weakest interaction, giving rise to a band at 3535 cm^{-1} is assigned to the O-H stretch-

Table 1. Infrared and Raman spectral data^a for L-ascorbic acid and sodium ascorbate.

L-Ascorbic acid			Sodium ascorbate			Tentative interpretation
Infrared	Raman		Infrared	Raman		
Solid ^b	Solid	Aq. solution	Solid ^b	Solid	Aq. solution	
3535 s						O-H str
3420 s						O-H str
3330 s			3320 s			O-H str
			3260 s			O-H str
3230 m						O-H str
			3170 w, bd			
3050 s, bd						O-H str
	3002 m					
	2978 m		2976 w	2978 s		
			2960 w	2965 m		
		2944 m, bd	2946 w	2954 m		C-H str
				2940 w		
2915 m, sp	2916 vs		2916 w	2925 vs	2933 s	
	2903 vs	2904 m, sp			2905 s	
2860 vw	2866 w	2863 vw	2850 vw			
2740 m, bd						O-H str
2650 w						
			2550 m, bd			
			2490 m, bd			
2340 w			2350 m			O-H str
			1702 vs	1704 vs	1717 vs	C=O str
1753 s	1754 w	1762 m, bd	1628 s			
			1595 vs	1598 vs, bd	1594 vs, bd	C=C str
1670 vs	1667 vs	1693 vs, bd				
1659 vs	1654 vs	1503 w				
			1482 m	1482 s		
1495 m	1498 m					
1482 w	1487 w	1470 m				
1455 m	1450 w		1450 m		1434 vw?	
1435 m			1404 w			
1385 β						CH ₂ scissor
1362 m	1372 w	1355 w	1359 m	1360 m	1360 m, bd	CH ₂ wag
	1344 vw			1330 s	1325 w	C-H def
1320 s	1321 s		1310 s, bd	1305 s	1295 s	O-H def
1300 vw	1297 m	1299 m				
1275 m			1271 s	1275 s	1280 s	
1248 w	1258 s	1273 vw		1247 w, bd	1242 m	
1220 m	1226 w	1218 m, bd	1231 s	1236 m		
1197 m	1200 m					
1138 s	1131 vs	1150 m	1156 s	1156 m	1142 m	C-O str
1118 s			1124 vs	1127 m	1114 m	
1110 s	1114 vw	1119 w				
1074 m		1087 vw	1072 vs	1077 s	1086 vw	
1065 m	1066 m	1052 m			1065 w	
1042 w	1039 vw		1048 s	1048 s	1043 s	C-C str
1025 s	1026 s	1022 w	1014 m	1015 s	1018 m	
988 s	993 w	981 vw	994 w		975 w, bd	
		937 m, bd	936 m	935 s	931 s	
869 m	872 m	873 m, bd	888 m	888 s	869 m	
820 m	822 s	826 vs	828 m	832 vs	832 vs	

Table 1. Continued.

756 s	742 w	797 vw	800 w		804 w, bd
721 m, bd		768 vw	752 s	757 m	762 w
711 vw	711 m			719 m	725 w, bd
675 m, bd	694 w		705 w, bd	707 s, bd	707 vs
		697 s			
		664 m	653 s	653 vs	669 s
629 m	629 s	633 s	601 s	604 vw	640 s
	589 s	589 m	583 s	585 m	605 vs
565 m	567 s	565 w, bd			
494 vw	490 w	488 w	493 w	496 w	490 m
473 w	477 m				
448 m	448 s	445 m, bd	424 s	427 m	437 m
		396 w, bd	380 m	383 vw	400 m, bd
			368 w	369 vw	
366 s	363 m				
350 s					
340 w	345 m		332 w	338 s	
292 w	295 m	305 w, bd	302 w	304 m	309 vs
	273 w			266 m	
	259 m				
238 m			240 w		
	223 m			227 w	
	208 m			194 vw	
	180 w			177 vw	
	163 m			163 vw	
	148 m				
	138 m			141 m	
	122 w			116 m	
	113 w			103 vw	
	91 m			94 s	
	81 s				
	73 s, sp			75 w, bd	
	43 vw			58 w	

^a Abbreviations used: s, strong; m, medium; w, weak; v, very; sp, sharp, and bd, broad.

^b The frequencies were observed in Nujol mulls (in KI-pellets for regions covered by Nujol bands).

ing vibration in the $O_6-H\cdots O_2^*$ bond where the $O\cdots O$ distance is 2.935 Å (the asterisk represents an atom in a neighbouring molecule). Unlike Kanters *et al.*¹⁴ we consider the structural and spectral data for this bond as evidence of a very weak hydrogen bond.

For the deuterated HASC it appears from Fig. 2 and Table 2 that six bands were observed which definitely can be assigned to hydrogen bonded O–D stretching modes. In NaASC there are three non-equivalent O–H \cdots O intermolecular linkages² which can be associated with the three O–H stretching frequencies at 3320, 3263, and 2350 cm^{-1} .

The assigned O–H stretching frequencies in HASC and NaASC have been correlated with the O–H \cdots O distances¹⁻³ and the results are plotted in Fig. 8. It appears that the experimental points can be fitted with a curve common to HASC and NaASC. This curve is compared with the experimental curve of Nakamoto *et al.*¹² constructed from 26 O \cdots O distances, assuming linear O–H \cdots O configurations. Our curve is significantly displaced towards higher frequencies (weaker interaction) compared with that of Nakamoto *et al.*

Table 2. Hydrogen bond distances and their correlated O–H (O–D) stretching frequencies for L-ascorbic acid (1–8) and for sodium ascorbate (a–c).

Bond ^a	Distance (Å)	Wave number (cm ⁻¹)	
		O–H	O–D
1 O6···O2'*	2.935	3535	2608
2 O5···O2'	2.786	3420	2537
3 O6*···O5'	2.769	3330	2470
4 O5*···O6	2.707	3230	2410
5 O3*···O1'*	2.666	3050	2270
6 O3···O1'	2.656		
7 O2*···O5'*	2.645		
8 O2···O6*	2.612	2740	2070
a O6···O1'''	2.820	3320	
b O5···O2''	2.709	3263	
c O2···O3'	2.546	2350	

^a Primes and asterisks refer to neighbouring molecules, Refs. 1–3.

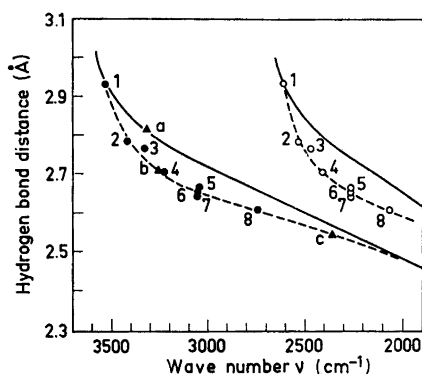


Fig. 8. Correlation chart of the crystallographic intermolecular O···O distance (Table 2) and the O–H (O–D) infrared stretching frequencies. (●, L-Ascorbic acid; ▲, sodium ascorbate; ○, deuterated L-ascorbic acid.) Solid curve for O–H from Ref. 11; the curve for O–D is constructed from the former using a factor 0.74.

This discrepancy may be caused¹² by the significant deviation from 180° in the present O–H–O angles³ (the deviations increase with the longer O···O distance).

The O–D frequencies in the deuterated HASC can easily be correlated with the corresponding O–H frequencies in the undeuterated sample. The ratio $\nu_{\text{O-D}}/\nu_{\text{O-H}}$ should be equal to 0.72 for a diatomic, harmonic oscillator, and was found close to 0.74 for the present molecules. In Fig. 8 the experimental points for the deuterated HASC have been plotted in an analogous way and Nakamoto's curve has been transformed to the O–D region, using the factor 0.74.

C–H, C=O, and C=C functional groups. With four carbon-hydrogen linkages in HASC and NaASC each molecule should have four C–H stretching bands. As apparent from Table 1, four infrared and Raman bands of solid HASC and NaASC were observed around 2900 cm⁻¹ and attributed to the C–H stretching modes.

From the structural analyses the following changes were observed¹⁻³ in the lactone ring system:

- (1) the $C_1=O_1$ distance was 0.017 Å shorter in HASC than in NaASC
- (2) the $C_2=C_3$ bond was 0.035 Å longer in NaASC and
- (3) the C_1-C_2 bond (connecting the $C_1=O_1$ and the $C_2=C_3$ bonds) was 0.036 Å shorter in NaASC. Thus, the conjugated $C_1=O_1$ and $C_2=C_3$ linkages both achieve more single bond character in NaASC than in HASC, whereas the central C_1-C_2 bond has more double bond character.

The spectral data agree with the structural parameters since the lactone $C=O$ stretching band at 1753 cm^{-1} in infrared (1754 cm^{-1} in Raman) for HASC corresponds to the 1702 cm^{-1} band (1704 cm^{-1} in Raman) in NaASC. An intense doublet around 1660 cm^{-1} was observed in infrared as well as in Raman for solid HASC and is attributed to the $C=C$ stretching mode. In NaASC very intense infrared and Raman bands around 1595 cm^{-1} reveal a much lower $C=C$ stretching vibration in this molecule.

CH₂ deformation and skeletal stretching region. Both HASC and NaASC have two hydrogen atoms linked to tertiary carbon atoms whereas two methylene hydrogens are attached to a secondary carbon atom. Various vibrational bands were observed in the region $1500-1200\text{ cm}^{-1}$ which are connected with the CH_2 scissoring, twisting, wagging and the $C-H$ deformation modes. The vibrations connected with a stretching of the $C-O-C$ group should be situated around 1100 cm^{-1} . Those mainly involving the $C-C$ vibrations in the ring and in the side chain are expected around 1000 cm^{-1} . However, the two $C-O$ and the four $C-C$ vibrations must be highly mixed for this molecule. Thus, the $C-C$ bond between sp^2 hybridized carbon atoms for which the stretching vibration should be considerably shifted to higher frequency in NaASC relative to HASC cannot easily be located in the spectra.

No definite correlation between the spectra of HASC and NaASC can be made below 900 cm^{-1} and the large number of infrared and Raman bands are connected with the different ring and side chain deformation modes. Various Raman bands were observed below 200 cm^{-1} in the solid samples. Some of these are undoubtedly low frequency internal vibrations, whereas others are external lattice vibrations.

Deuterated ascorbic acid. A comparison between Fig. 1 and Fig. 2 reveals that the stronger bands in HASC are still present in the deuterated sample. In particular, the hydrogen bonded $O-H$ stretching bands are present, in addition to the $O-D$ bands. Thus, our present spectroscopic results support the previous conclusions from the neutron diffraction study that the exchange of hydroxyl protons with deuterium was incomplete. The extent of exchange was there found to be 42 % in all the hydroxyl positions, but no exchange was found to take place at the $C-H$ sites. This is in sharp contradiction to earlier reports⁷ that such an exchange readily occurred. That conclusion was partly based upon an assignment of the 3034 cm^{-1} band to a $C-H$ stretching frequency, while we assign this broad absorption to three overlapping $O-H$ stretching bands.

The spectrum in Fig. 2 is obtained from the very crystal used in the neutron diffraction analysis. Some of our samples made more recently reveal a higher

degree of isotopic exchange as inferred from the intensities of the O–D relative to the O–H stretching bands. The spectra indicate an isotopic ratio between 40 and 60 % in all the hydroxyl sites.

Solution spectra

It appears from Figs. 5–7 and from Table 1 that various changes occurred in the Raman spectra when the crystalline solids were dissolved in water. Thus, the solution spectra were less complete than those of the solids and very weak Raman bands were not observed in solution. More important, various structural and chemical conclusions can be drawn from a comparison between the crystalline and the solute spectra. Since no large variations are observed, it seems obvious that no drastic rearrangement of the rings *etc.* occurs in aqueous solution compared with the crystal. On the other hand, each molecule of HASC or NaASC will be strongly affected by hydrogen bonding to the water molecules. Since we were not able to cover the region above 3000 cm^{-1} in Raman with our red laser, no direct evidence for the solute-solvent interaction can be obtained from the OH stretching region.

The C=O and the C=C stretching bands in HASC were both shifted to higher frequencies in aqueous solution, indicating higher double bond character. For NaASC the C=O band was blue shifted and the C=C band slightly red shifted in solution. A large number of minor frequency shifts from solid to aqueous solution were detected below 1500 cm^{-1} . These shifts are expected for various reasons, including change from the crystalline to the dissolved state, the high dielectric constant of water and the solute-solvent interaction affecting in particular the O–H deformation modes. Moreover, the low frequency Raman bands of HASC and NaASC in aqueous solution appeared broad compared with the solid state bands. This observation can be attributed to the less defined conformation of the side chain in solution relative to the crystal. The breaking up of intermolecular hydrogen bonds upon solution and the formation of solute-solvent bonds would have a pronounced effect upon the geometry of the side chain. Particularly the low frequency skeletal modes will be affected by conformational changes, resulting in broad, diffuse vibrational bands.

Protolytic equilibrium. HASC is an intermediately strong acid ($\text{p}K_1 = 4.26$; $\text{p}K_2 = 11.64$) in aqueous solution. Accordingly, the aqueous solutions of HASC or NaASC should contain predominantly the species HASC or ASC^- , respectively. The protolytic equilibrium of HASC in aqueous solution was studied by means of the Raman spectra. In a saturated solution of HASC the pH was adjusted to 0 by adding HCl, and correspondingly the pH in an NaASC solution was adjusted to 9 by adding NaOH. The Raman spectra of these solutions were identical to those obtained from the HASC and NaASC solutions, respectively. Further studies were made by adding NaOH to a saturated solution of HASC until $\text{pH} = \text{p}K_2$. The observed Raman spectrum turned out to be a superposition of the HASC and the NaASC spectra in agreement with the predicted equal concentrations of HASC and ASC^- at this pH.

We are indebted to Mrs. Wiltrud Rademacher for recording some of the spectra, and to Mrs. Moj Bonnevie-Svendsen for analyzing the sample of heavy water.

REFERENCES

1. Hvoslef, J. *Acta Cryst. B* **24** (1968) 23.
2. Hvoslef, J. *Acta Cryst. B* **25** (1969) 2214.
3. Hvoslef, J. *Acta Cryst. B* **24** (1968) 1431.
4. Williams, D. and Rogers, L. H. *J. Am. Chem. Soc.* **59** (1937) 1422.
5. Heintz, E. *Compt. Rend.* **208** (1939) 1893.
6. Trotter, I. F., Thompson, H. W. and Wokes, F. *Biochem. J.* **42** (1942) 601.
7. Weigl, J. W. *Anal. Chem.* **24** (1952) 1483.
8. Edsall, J. T. and Sagall, E. L. *J. Am. Chem. Soc.* **65** (1943) 1312.
9. Kresheck, G. C. *Biochem. Biophys. Res. Commun.* **33** (1968) 374.
10. Pimentel, G. C. and McClellan, A. L. *The Hydrogen Bond*, Freeman, San Francisco 1960.
11. Arnett, E. M., Joris, L., Mitchell, E., Murty, T. S. S. R., Gorrie, T. M. and Schleyer, P. v. R. *J. Am. Chem. Soc.* **92** (1970) 2365.
12. Nakamoto, K., Margoshes, M. and Rundle, R. E. *J. Am. Chem. Soc.* **77** (1955) 6480.
13. Pimentel, G. C. and Sederholm, C. H. *J. Chem. Phys.* **24** (1956) 639.
14. Kanters, J. A., Kroon, J., Peerdeman, A. F. and Vliegthart, J. A. *Nature* **222** (1969) 370.

Received January 22, 1971.